Bubble nucleation at zero and nonzero temperatures

Mario Gutierrez Abed[1, *] and Ian G. Moss[1, †]

[1]*School of Mathematics, Statistics and Physics,*

Newcastle University, Newcastle Upon Tyne, NE1 7RU, UK

(Dated: July 16, 2020)

The theory of false vacuum decay in a thermal system may have a cross-over from predominantly thermal transitions to quantum transitions as the temperature is decreased. New numerical methods and results are presented here that can be used to model thermal and vacuum bubble nucleation in this regime for cosmology and for laboratory analogues of early universe phase transitions.

I. INTRODUCTION

The early evolution of our universe is mostly a story of large scale homogeneity with small scale perturbative fluctuations. Occasionally, though, non-perturbative effects may have played a role during first order phase transitions. Characteristic features include the nucleation of bubbles, possibly involving periods of extreme supercooling into a metastable, false vacuum state. Bubble formation can be predominantly a quantum, or predominantly a thermal process. In this paper we investigate the cross-over from thermal to vacuum nucleation in systems with first order transitions.

Bubble nucleation in a thermal system can be described in terms of instantons, solutions to an effective field theory with imaginary time coordinate [1–3]. The thermal aspect of the decay is represented by imposing periodicity in the imaginary time coordinate, with period $\beta = \hbar/(k_B T)$. At low temperatures, the size of the instanton is small compared to β and thermal effects appear mostly through the form of the effective potential [3]. At higher temperatures, provided the effective potential still has a potential barrier, the instanton solution becomes constant in the imaginary time direction. In between, there is a cross-over region were instanton solutions become distorted.

---

* M.L.Gutierrez-Abed2@newcastle.ac.uk

† ian.moss@newcastle.ac.uk

Interest in vacuum decay has been rekindled in the past few years by the possibility that the process could be simulated in a laboratory Bose Einstein condensate [4–7]. These systems will allow the first experimental tests of the theoretical framework used to describe early universe phase transitions. It will be necessary to perform precise numerical modelling to compare theory with experimental results. Bubble nucleation rates in cosmology are usually obtained using shooting methods (e.g. [8, 9]). We will present a new numerical method for calculating nucleation exponents for thermal vacuum decay applicable to the regime where both both thermal and vacuum effects are important, and the shooting methods cannot be used. This method can also be used when there is a background, or nucleation seed, and it has already been used to obtain the results in Ref. [10], but the method was not explained previously.

II. THE MODEL

We use a model based on the spinor BEC system of Fialko et al. [4], where the relative phase between the wave-functions of two atomic states φ is described by an action

$$S = \chi \int d^n x dt \left\{ \frac{1}{2}\dot{\varphi}^2 - \frac{1}{2}(\nabla\varphi)^2 - V(\varphi) \right\}. \tag{1}$$

Natural length and time units have been chosen based on the underlying physics (explained later), and the parameter χ contains the remaining dependence on physical parameters. The potential has been scaled to the form

$$V(\varphi) = -(1 + \cos\varphi) + \frac{1}{2}\lambda^2 \sin^2\varphi. \tag{2}$$

This potential has has two minima, a true vacuum at $\varphi = 0$ and a false vacuum at $\varphi = \pi$, separated by a potential barrier whose height depends on the parameter λ. The number of spatial dimensions, n, depends on the details of the experiment, and we will consider $n = 1 \ldots 3$. The motivation for this potential is based on a particular BEC system, but it also serves as a toy model for early universe false vacuum decay, the essential features being that the system has a relativistic dispersion relation, and the potential has the two minima separated by a potential barrier.

In a thermal system, the field responds to a modified potential that has $\lambda \equiv \lambda(T)$ [15]. In an early universe setting, this effect plays an important role in placing the field in the false

vacuum as the universe supercools. In a laboratory setting, the phase is prepared in the false vacuum as part of the experimental protocol. The potential barrier in the analogue model is still present at zero temperature, and the temperature dependence of the potential plays far less of a role than it would in some particle models. We will take λ to be constant in the modelling, and comment on temperature dependent parameters later.

The first-order false vacuum decay is a non-perturbative process, in which quantum and thermal effects can contribute. In either case, the decay can be described by an instanton solution φ_b to the field equations with imaginary time τ.

$$\frac{\partial^2 \varphi}{\partial \tau^2} + \nabla^2 \varphi - \frac{\partial V}{\partial \varphi} = 0 \tag{3}$$

In the vacuum case, the field approaches the false vacuum value as $\tau \to \pm\infty$. In the thermal case, an initial thermal ensemble is represented by solutions that are periodic in τ with period $\beta = 1/T$. We will refer to the special case of an instanton solution which is independent of τ as a quasi-static instanton.

The full expression for the nucleation rate of vacuum bubbles in a volume $\mathcal{V}$ depends on the Euclidean action $S_E = iS$ of the instanton solution. According to Coleman [1, 2],

$$\Gamma \approx \mathcal{V} \left| \frac{\det' S_E''[\varphi_b]}{\det S_E''[\varphi_{\text{fv}}]} \right|^{-1/2} \left(\frac{S_E[\varphi_b]}{2\pi} \right)^{N/2} e^{-S_E[\varphi_b]}. \tag{4}$$

where S_E'' denotes the second functional derivative of the Euclidean action, and $\det'$ denotes omission of $N = n + 1$ zero modes from the functional determinant of the operator in the vacuum case and $N = n$ zero modes for the quasi-static instanton. The translational symmetry of the underlying theory is broken by the instanton, and the zero modes are the modes representing translations.

The action for a quasi-static instanton in one spatial dimension can be obtained analytically and provides a test for the numerical results we obtain later. In this case, the solution $\varphi \equiv \varphi(x)$ satisfies

$$\frac{d^2 \varphi}{dx^2} - \frac{\partial V}{\partial \varphi} = 0, \tag{5}$$

with $\varphi \to \pi$ as $x \to -\infty$. This first integral of motion implies $d\varphi/dx = (2V)^{1/2}$, and the solution bounces off the potential at $\varphi_r = \arccos(1 - 2/\lambda^2)$. The action S_E is

$$S_E = 2\chi\beta \int_{\varphi_r}^{\pi} d\varphi \, (2V)^{1/2}. \tag{6}$$

The integral can be obtained in closed form,

$$S_E = 4\chi\beta \left\{ (\lambda^2 - 1)^{1/2} - \lambda^{-1} \ln \left[(\lambda^2 - 1)^{1/2} + \lambda \right] \right\} \tag{7}$$

This exact solution is no longer valid in dimensions two and three, but it can be adapted, for large λ, using the thin-wall approximation discussed below.

The vacuum instanton in one spatial dimension has $O(2)$ symmetry, and the solution is a function of $r = |\mathbf{x}|$. In the thin-wall approximation, the solution remains close to the true vacuum value for small r, until a value $r \approx R$, when the solution changes rapidly over a short distance (the 'wall') with $d\varphi/dr \approx (2V)^{1/2}$. The Euclidean action in two dimensions can be approximated by splitting it up into the interior and the wall,

$$S_E \approx -2\pi R^2 \chi + 4\pi\chi R\lambda \tag{8}$$

There is an extremum at $R = \lambda$, where $S_E \approx 2\pi\chi\lambda$. For small temperatures, this is lower than the quasi-static action form Eq. (7), $S_E \approx 4\chi\beta\lambda$. In the thin wall approximation, vacuum tunnelling dominates at temperatures below $T \approx 2/\pi$, and thermal tunnelling dominates at higher temperatures.

The thin-wall approximation is only valid when the potential barrier is relatively large. In a laboratory analogue of vacuum decay, large barriers would be associated with bubble nucleation rates too small to be seen in the experiment. In the next section we look at new methods for evaluating the action that can go beyond the thin-wall approximation.

The behaviour of the pre-factor in the nucleation rate (4) can be analysed by different numerical methods which we will not attempt to investigate here [11–13]. We note only that, since we are not in the thin-wall limit, there are no small parameters in the problem, and so we expect the pre-factor to be of order one in the length and time units that have been used in the action.

III. NUMERICAL METHOD

The instanton solution for false vacuum decay in n spatial dimensions has $O(n + 1)$ symmetry, allowing the instanton equation to be reduced to an ordinary differential equation that is easily solved using shooting methods [11]. The reduced symmetry for the instantons in crossover regime of the thermal problem bars the use of this method. Although the instanton

equations are a well-posed elliptic system, the negative and zero modes in $S_E''[\varphi_b]$ can be problematic for standard numerical techniques. We present a new relaxation method that overcomes these problems.

The basic relaxation method for solving a set of equations $S_E'[\varphi] = 0$ introduces a field Φ that depends on $\mathbf{x}$, τ and a relaxation time s. The field Φ solves

$$\frac{d\Phi}{ds} = -\mathcal{O}S_E'[\Phi], \tag{9}$$

where the operator $\mathcal{O}$ is introduced to optimise convergence to the solution, $\Phi \to \varphi_b$ as $s \to \infty$. Close to the instanton solution, the behaviour of Φ is governed by the second order operator $S_E''[\varphi_b]$. If the solution to the relaxation equation is $\Phi = \varphi_b + \delta\varphi$, then the relaxation scheme for $\delta\varphi$ small reduces to

$$\frac{d\delta\varphi}{ds} = -\mathcal{O}S_E''[\varphi_b]\delta\varphi. \tag{10}$$

Choosing $\mathcal{O}$ so that $\mathcal{O}S_E''[\varphi_b]$ has a positive spectrum leads to convergence in a neighbourhood of the solution. Since $S_E''[\varphi_b]$ has a negative eigenvalue, we cannot choose $\mathcal{O}$ to be a multiple of the identity. The choice $\mathcal{O} = (S_E''[\Phi])^{-1}$ gives convergence, but it requires a matrix inversion step that may itself be problematic due to small eigenvalues of the operator.

A simple stability analysis by the von Neumann method shows that another obvious choice $\mathcal{O} = (S_E''[\varphi])^\dagger$ requires a very small numerical relaxation time step. For a spatial step size Δx, $\Delta s = O(\Delta x^4)$ for stability. However, this can be improved by taking a second order equation in the relaxation time,

$$\frac{d^2\Phi}{ds^2} + 2k\frac{d\Phi}{ds} + (S_E''[\phi])^\dagger S_E'[\phi] = 0, \tag{11}$$

with a new parameter, the damping coefficient k. Using central differencing for the relaxation time derivatives, stability now requires $\Delta s = O(\Delta x^2)$.

The method works provided the initial guess for the bubble profile is sufficiently close to the final solution. In practice, a shape based on the thin-wall approximation serves well. If the initial bubble radius is too small, then Φ relaxes to the false vacuum state and a larger initial radius has to be selected.

The convergence of the method is related to the eigenvalue spectrum of $S_E''[\phi]$. If we consider a single mode with eigenvalue ν, then the amplitude $\delta\varphi_\nu$ of the mode decays exponentially,

$$\delta\varphi_\nu \propto e^{-ks + (k^2 - |\nu|^2)^{1/2}s} \tag{12}$$

The zero modes are an exception, but the boundary conditions can be chosen to 'pin' the centre of the instanton at the corner of the integration region to remove the (translational) zero modes. For large values of $|\nu|$, the convergence is determined by k, and for small $|\nu|$, by $|\nu|^2/(2k)$. The optimal value of k would therefore be $k \approx |\nu_{\min}|$, where $\nu_{\min}$ is the eigenvalue with smallest modulus

IV. RESULTS

Numerical results for the field of a non-static and quasi-static instanton solutions in one dimension are shown in figure 1. At low temperatures, the non-static instanton approximates the $O(2)$ symmetric vacuum instanton. At higher temperatures, in this case around $T = 0.125$, the non-static instanton becomes distorted in the imaginary time direction. The quasi-static instanton solution is also shown. The radius of the instantons in the spatial direction, defined as the distance to the average field value, is between 2 and 3 length units.
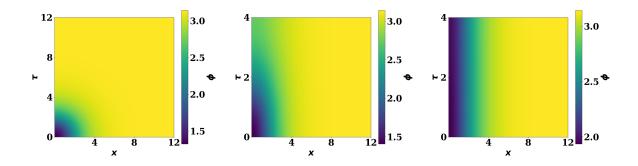

Figure 1. These plots show the value of φ_b for shallow instantons in one dimension. Left: The $O(2)$ symmetric vacuum instanton. Middle: The non-static instanton at $T = 0.125$. Right: The quasi-static instanton at $T = 0.125$. In all cases $\lambda = 1.2$.

Values of the Euclidean action at different temperatures are plotted in figure 3. At low temperatures, the non-static instanton has the lowest action. There is a crossover point where the non-static solution merges into the quasi-static solution. We did not find any evidence for a non-static solution with higher action than the quasi-static solution.
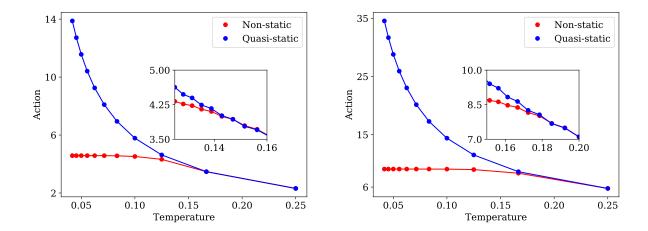
Figure 2. The plots show the dependence of the Euclidean action on temperature for non-static and quasi-static instantons with different potential barrier heights. Left: $\lambda = 1.2$; right: $\lambda = 1.4$.
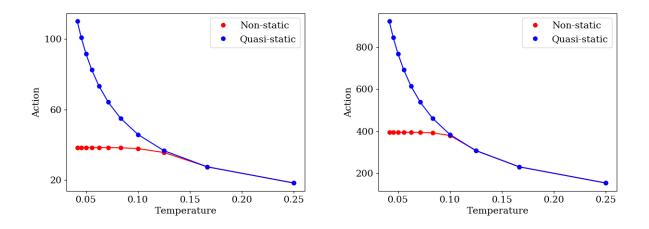

Figure 3. The plots show the dependence of the Euclidean action on temperature for non-static and quasi-static instantons. Left: two dimensions; right: three dimensions. In both cases $\lambda = 1.2$

In figure 4, we have taken the general form of the action for a quasi-static instanton and parameterised this by

$$S_E = \chi \alpha_n(\lambda)\beta, \tag{13}$$

in n spatial dimensions. The vacuum instanton has action

$$S_E = \chi \alpha_{n+1}(\lambda), \tag{14}$$

In one dimension, the agreement between the numerical values of α_n and the analytic

expression Eq (7) is excellent. In two and three dimensions, the results differ substantially from the thin wall approximation. A numerical fit is shown instead.
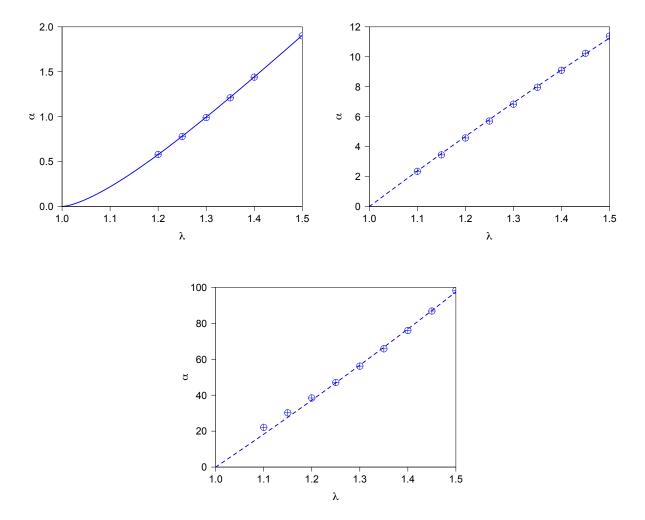

Figure 4. Values of α_n that determine the tunnelling exponent for the quasi-static instanton in $S_E = \chi \alpha_n(\lambda)\beta$. The first plot is for one dimension and also shows the exact analytic result using expression Eq. (7). The second and third plots for two and three dimensions superimpose a numerical fit $a_1(x-1) + a_2(x-1)^2$. In two dimensions $(a_1, a_2) = (24.0, -3.0)$ and in three dimensions $(a_1, a_2) = (180, 30.0)$

V.   CONCLUSION

We have investigated the cross-over regime of bubble nucleation where the tunnelling instantons that dominate the nucleation rate lose one degree of symmetry. The numerical results were obtained using a new numerical method. We found that the distorted instantons merge smoothly into quasi-static instantons.

The results have been expressed in terms of a natural set of units which are adaptable to the system under consideration. In the case of the spinor gas, for example, the system has a characteristic healing length ξ and natural frequency ω_0 [4]. The strength of the coupling between the spin states is tunable, and fixed by a small parameter ϵ. The units used for the numerical modelling are the length unit $\xi/(2\epsilon)$ and the temperature unit $2\hbar\omega_0\epsilon/k_B$. The factor in front of the action (1) in n dimensions is

$$\chi = 2^{-n}\epsilon^{1-n}\rho\,\xi^n, \tag{15}$$

where ρ is the number density of atoms. In the example from Ref. [4], taking 5×10^5 atoms of ^{7}Li in a one dimensional atomic trap of length 120μm, the length unit would be $0.1\epsilon^{-1}\mu$m and the temperature unit 12ϵ mK.

The analogue system has an asymmetric double well potential in the zero temperature limit. There are models in particle physics with this behaviour, for example the high-energy Higgs models used to discuss stability of the Higgs vacuum [14–18]. On the other hand, there are situations, such as variants of the standard model of particle physics where the electroweak transition is first order, in which the potential barrier disappears at zero temperature [19–21]. Our numerical methods can only be extended to these situations by taking into account the temperature dependence in the parameters $\chi(T)$ and $\lambda(T)$. It would then be of interest to check, in each particular model, whether the crossover between the different instanton types occurs before the transition is completed.

[1] Sidney R. Coleman, "The Fate of the False Vacuum. 1. Semiclassical Theory," Phys. Rev. **D15**, 2929–2936 (1977), [Erratum: Phys. Rev.D16,1248(1977)].

[2] Curtis G. Callan and Sidney R. Coleman, "The Fate of the False Vacuum. 2. First Quantum Corrections," Phys. Rev. **D16**, 1762–1768 (1977).

[3] A.D. Linde, "Decay of the false vacuum at finite temperature," Nuclear Physics B **216**, 421 – 445 (1983).

[4] O. Fialko, B. Opanchuk, A. I. Sidorov, P. D. Drummond, and J. Brand, "Fate of the false vacuum: Towards realization with ultra-cold atoms," EPL (Europhysics Letters) **110**, 56001 (2015), arXiv:1408.1163 [cond-mat.quant-gas].

[5] Jonathan Braden, Matthew C. Johnson, Hiranya V. Peiris, and Silke Weinfurtner, "Towards the cold atom analog false vacuum," JHEP **07**, 014 (2018), arXiv:1712.02356 [hep-th].

[6] Jonathan Braden, Matthew C. Johnson, Hiranya V. Peiris, Andrew Pontzen, and Silke Weinfurtner, "New Semiclassical Picture of Vacuum Decay," Phys. Rev. Lett. **123**, 031601 (2019), arXiv:1806.06069 [hep-th].

[7] Jonathan Braden, Matthew C. Johnson, Hiranya V. Peiris, Andrew Pontzen, and Silke Weinfurtner, "Nonlinear Dynamics of the Cold Atom Analog False Vacuum," JHEP **10**, 174 (2019), arXiv:1904.07873 [hep-th].

[8] Greg W. Anderson and Lawrence J. Hall, "Electroweak phase transition and baryogenesis," Phys. Rev. D **45**, 2685–2698 (1992).

[9] Ariel Megevand and Santiago Ramrirez, "Bubble nucleation and growth in very strong cosmological phase transitions," Nuclear Physics B **919**, 74 – 109 (2017).

[10] Thomas P. Billam, Ruth Gregory, Florent Michel, and Ian G. Moss, "Simulating seeded vacuum decay in a cold atom system," Phys. Rev. D **100**, 065016 (2019), arXiv:1811.09169 [hep-th].

[11] Sidney Coleman, *Aspects of Symmetry: Selected Erice Lectures* (Cambridge University Press, Cambridge, U.K., 1985).

[12] Bjorn Garbrecht and Peter Millington, "Self-consistent solitons for vacuum decay in radiatively generated potentials," Phys. Rev. D **92**, 125022 (2015), arXiv:1509.08480 [hep-ph].

[13] Wen-Yuan Ai, Björn Garbrecht, and Carlos Tamarit, "Functional methods for false-vacuum decay in real time," Journal of High Energy Physics **2019** (2019), 10.1007/jhep12(2019)095.

[14] A. D. Linde, "On the Vacuum Instability and the Higgs Meson Mass," Phys. Lett. **B434**, 306 (1977).

[15] M. Sher, "Electroweak Higgs Potentials and Vacuum Stability," Phys. Rept. **179**, 273 (1989).

[16] Giuseppe Degrassi, Stefano Di Vita, Joan Elias-Miro, Jose R. Espinosa, Gian F. Giudice, Gino Isidori, and Alessandro Strumia, "Higgs mass and vacuum stability in the Standard Model at NNLO," JHEP **08**, 098 (2012), arXiv:1205.6497 [hep-ph].

[17] Vincenzo Branchina and Emanuele Messina, "Stability, Higgs Boson Mass and New Physics," Phys.Rev.Lett. **111**, 241801 (2013), arXiv:1307.5193 [hep-ph].

[18] Vincenzo Branchina, Emanuele Messina, and Marc Sher, "Lifetime of the electroweak vacuum and sensitivity to Planck scale physics," Phys.Rev. **D91**, 013003 (2015), arXiv:1408.5302 [hep-ph].

[19] Yoshihiro Kondo, Isao Umemura, and Katsuji Yamamoto, "First order phase transition in the singlet Majoron model," Phys. Lett. B **263**, 93–96 (1991).

[20] K. Kajantie, M. Laine, K. Rummukainen, and Mikhail E. Shaposhnikov, "A Nonperturbative analysis of the finite T phase transition in SU(2) x U(1) electroweak theory," Nucl. Phys. B **493**, 413–438 (1997), arXiv:hep-lat/9612006.

[21] J.R. Espinosa, T. Konstandin, and F. Riva, "Strong electroweak phase transitions in the standard model with a singlet," Nuclear Physics B **854**, 592 – 630 (2012).